Article

Syntheses, Structures, Spectroscopic Properties, and π-Dimeric Interactions of [*n*.*n*]Quinquethiophenophanes

Toyofumi Sakai, Teizi Satou, Takeshi Kaikawa, Kazuo Takimiya, Tetsuo Otsubo, and Yoshio Aso

J. Am. Chem. Soc., **2005**, 127 (22), 8082-8089• DOI: 10.1021/ja050783u • Publication Date (Web): 14 May 2005

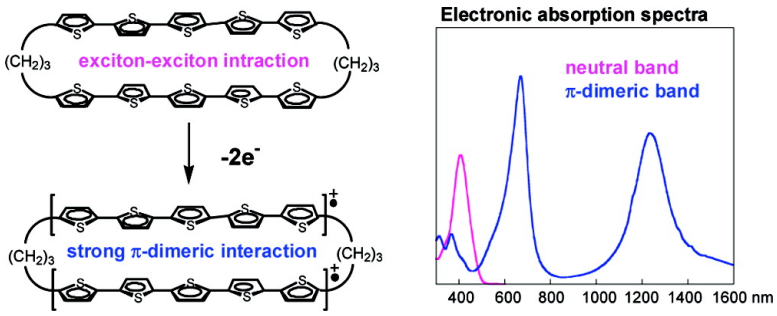

More About This Article

Additional resources and features associated with this article are available within the HTML version:

- Supporting Information
- Links to the 13 articles that cite this article, as of the time of this article download
- Access to high resolution figures
- Links to articles and content related to this article
- Copyright permission to reproduce figures and/or text from this article

View the Full Text HTML

J|A|C|S
ARTICLES
Published on Web 05/14/2005

Syntheses, Structures, Spectroscopic Properties, and π-Dimeric Interactions of [*n.n*]Quinquethiophenophanes

Toyofumi Sakai,[†] Teizi Satou,[†] Takeshi Kaikawa,[†] Kazuo Takimiya,[†] Tetsuo Otsubo,*[,†] and Yoshio Aso[‡]

Contribution from the Department of Applied Chemistry, Graduate School of Engineering, Hiroshima University, Higashi-Hiroshima 739-8527, Japan, and The Institute of Scientific and Industrial Research, Osaka University, CREST, Japan Science and Technology Agency (JST), Ibraki, Osaka 567-0047, Japan

Received February 6, 2005; E-mail: otsubo@hiroshima-u.ac.jp

Abstract: A cyclophane-type of dimeric quinquethiophenes (**4a**−**e**) with the bridge chains consecutively varying from two to six methylenes has been synthesized and studied as ideal π-dimer models. The double-decker structures of these compounds are verified by upfield shifts for the proton NMR signals of the inside thiophenes, as compared to those of monomeric dimethylquinquethiophene (**3**). The electronic absorption and emission spectra of **4a**−**e** are perturbed by through-space π-electronic interactions involving exciton−exciton coupling between the two overlapped quinquethiophenes, which become marked with shortening of the bridged alkylene chains. One-electron oxidation of **4a**−**e** with $FeCl_3$ in dichloromethane results in the appearance of specific polaronic bands in the near-infrared region of the electronic absorption spectra, due to the generation of a radical cation species (polaron) on one of the quinquethiophenes, which electronically interacts with the remaining neutral species. Two-electron oxidation of **4a**−**e** introduces spectral changes, revealing that the resulting two quinquethiophene radical cations readily form an intramolecular π-dimer, thanks to their close stacking, in contrast to the difficult formation of an intermolecular π-dimer from **3**. The π-dimeric spectra of **4b**−**e** are comprised of two strong absorption bands, similar to that of **3**, the low-energy band of which is considerably red-shifted by an effective π-dimeric interaction depending on the lengths of the bridged alkylene chains. Quite different is the spectrum of **4a** with three absorption bands inherent in π-dimer, presumably because the two short bridging chains of **4a** force the π-dimer to take a constrained, strongly interactive structure.

Introduction

The principal charge carriers of conductive polyaromatics, such as polythiophenes, polypyrroles, and polyanilines, were initially considered to be a radical cation species termed polaron, which is stabilized by charge delocalization over a sequence of several linked aromatic units.[1] However, ESR inactivity for deeply doped polymers suggested the involvement of spinless dimeric species formed by a combination of two polarons.[2] Various types of dimeric species, such as bipolaron,[1,2] π-dimer,[3−10] chain dimer,[11] and σ-dimer,[12] have been so far proposed, and among them, π-dimer species has been most supported by many documents, principally based on the spectral studies of appropriate oligomers in solution in high concentrations or at low temperatures.[4,6−9] However, because of the incomplete formation

[†] Hiroshima University.
[‡] Osaka University.

(1) Brédas, J. L.; Street, G. B. *Acc. Chem. Res*. **1985**, *18*, 309−315.
(2) Heeger, A. J.; Kivelson, S.; Schrieffer, J. R.; Su, W. P. *Rev. Mod. Phys.* **1998**, *60*, 781−860.
(3) Miller, L. L.; Mann, K. R. *Acc. Chem. Res*. **1996**, *29*, 417−423.
(4) (a) Hill, M. G.; Mann, K. R.; Miller, L. L.; Penneau, J.-F. *J. Am. Chem. Soc.* **1992**, *114*, 2728−2730. (b) Hill, M. G.; Penneau, J.-F.; Zinger, B.; Mann, K. R.; Miller, L. L. *Chem. Mater*. **1992**, *4*, 1106−1113. (c) Zinger, B.; Mann, K. R.; Hill, M. G.; Miller, L. L. *Chem. Mater*. **1992**, *4*, 1113−1118. (d) Miller, L. L.; Yu, Y.; Gunic, E.; Duan, R. *Adv. Mater*. **1995**, *7*, 547−548. (e) Yu, Y.; Gunic, E.; Zinger, B.; Miller, L. L. *J. Am. Chem. Soc*. **1996**, *118*, 1013−1018. (f) Graf, D. D.; Duan, R. G.; Campbell, J. P.; Miller, L. L.; Mann, K. R. *J. Am. Chem. Soc*. **1997**, *119*, 5888−5899.
(5) Zotti, G.; Schiavon, G.; Berlin, A.; Pagani, G. *Chem. Mater*. **1993**, *5*, 620−624.
(6) (a) Bäuerle, P.; Segelbacher, U.; Gaudl, K.-U.; Huttenlocher, D.; Mehring, M. *Angew. Chem., Int. Ed. Engl.* **1993**, *32*, 76−78. (b) Bäuerle, P.; Segelbacher, U.; Maier, A.; Mehring, M. *J. Am. Chem. Soc*. **1993**, *115*, 10217−10223. (c) Segelbacher, U.; Sariciftci, N. S.; Grupp, A.; Bäuerle, P.; Mehring, M. *Synth. Met.* **1993**, *57*, 4728−4733.
(7) (a) Audebert, P.; Hapiot, P.; Pernaut, J.-M.; Garcia, P. *J. Electroanal. Chem.* **1993**, *361*, 283−287. (b) Hapiot, P.; Audebert, P.; Monnier, K.; Pernaut, J.-M.; Garcia, P. *Chem. Mater*. **1994**, *6*, 1549−1555. (c) Audebert, P.; Hapiot, P. *Synth. Met.* **1995**, *75*, 95−102.
(8) Apperloo, J. J.; Groenendaal, L. B.; Verheyen, H.; Jayakannan, M.; Janssen, R. A. J.; Dkhissi, A.; Beljonne, D.; Lazzaroni, R.; Brédas, J.-L. *Chem. Eur. J.* **2002**, *8*, 2384−2396.
(9) Raimundo, J.-M.; Levillain, E.; Gallego-Planas, N.; Roncali, J. *Electrochem. Commun.* **2000**, *2*, 211−215.
(10) (a) Rossi, L.; Lanzani, G.; Garnier, F. *Phys. Rev. B* **1998**, *58*, 6684−6687. (b) Casado, J.; Bengoechea, M.; Navarrete, J. T. L.; Otero, T. F. *Synth. Met.* **1998**, *95*, 93−100.
(11) (a) Tol, A. J. W. *Chem. Phys.* **1996**, *208*, 73−79. (b) van Haare, J. A. E. H.; Havinga, E. E.; van Dongen, J. L. J.; Janssen, R. A. J.; Cornil, J.; Brédas, J.-L. *Chem. Eur. J.* **1998**, *4*, 1509−1522. (c) Apperloo, J. J.; Janssen, R. A. J.; Malenfant, P. R. L.; Groenendaal, L.; Fréchet, J. M. J. *J. Am. Chem. Soc.* **2000**, *122*, 7042−7051. (d) Gao, Y.; Liu, C.-G.; Jiang, Y.-S. *J. Phys. Chem. A* **2002**, *106*, 5380−5384. (e) Geskin, V. M.; Brédas, J.-L. *ChemPhysChem*. **2003**, *4*, 498−505.
(12) (a) Yu, Y.; Gunic, E.; Miller, L. L. *Chem. Mater*. **1995**, *7*, 255−256. (b) Smie, A.; Heinze, J. *Angew. Chem., Int. Ed.* **1997**, *36*, 363−367. (c) Tschuncky, P.; Heinz, J.; Smie, A.; Engelmann, G.; Kossmehl, G. *J. Electoanal. Chem.* **1997**, *433*, 223−226. (d) Heinze, J.; Tschuncky, P.; Smie, A. *J. Solid State Electrochem.* **1998**, *2*, 102−109. (e) Engelmann, G.; Kossmehl, G.; Heinze, J.; Tschuncky, P.; Jugelt, W.; Welzel, H.-P. *J. Chem. Soc., Perkin Trans. 2* **1998**, 169−175. (f) Heinze, J.; John, H.; Dietrich, M.; Tschuncky, P. *Synth. Met*. **2001**, *119*, 49−52.

10.1021/ja050783u CCC: $30.25

Scheme 1 [a]

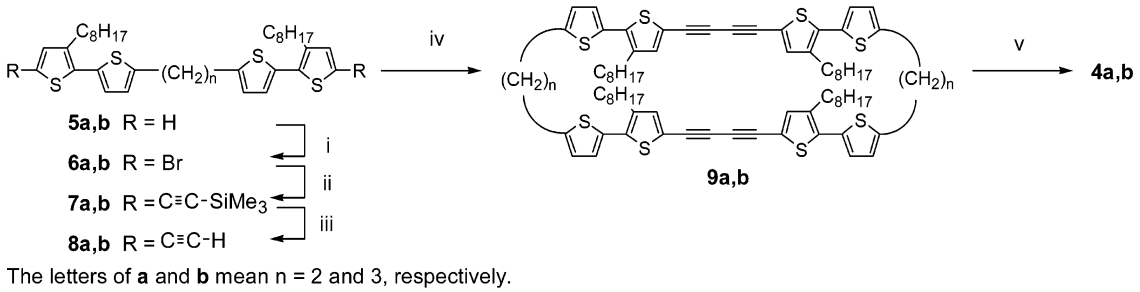

[a] Reagents and conditions: (i) 2 equiv of NBS (89−93%); (ii) (trimethylsilyl)acetylene, $Pd(PPh_3)_4$, CuI, Et_3N (97%); (iii) KOH−MeOH (93%−quant.); (iv) $Cu(OAc)_2$, pyridine (**9a**, 22%; **9b**, 9%); (v) $Na_2S{\cdot}H_2O$ (**4a**, 41%; **4b**, 17%).

and/or weak interactions of π-dimers from oligomers, it is rare to be able to detect the intrinsic absorption bands of π-dimers involving an interchain transition polarized along the stacking axis.[4e,13] The studies of π-dimers using oligomers were also carried out in the film state[5,10] or in the crystal state.[4f,14] In the expectation that well-characterized, extraordinarily long oligomers are more suitable models to clarify the ambiguous doping properties of polymers, we systematically studied a series of long oligothiophenes (**1**) up to the 48-mer.[15] The electrical conductivities of the oligothiophenes under doping gradually approach those of polythiophenes as the thiophene units increase, and their spectroscopic analyses suggested the involvement of π-dimers as charge carrier species.[16] As another approach to the elucidation of π-dimers, we also studied dimeric oligothiophenes (**2a**−**e**) linked with a single alkylene chain.[17] Although they do not take any stacked structure in the neutral state, compounds **2b**−**e** in the oxizided state readily give π-dimers, when compared to difficult intermolecular π-dimerization of monomeric dimethyldioctylquinquethiophene (**3**). However, the first member with an ethylene chain (**2a**) could not stack intramolecularly, because of severe strain accompanied by the molecular bending. As more suitable π-dimer models, we have focused on a cyclophane type of dimeric quinquethiophenes **4a**−**e**, where the double linkages force the two quinquethiophene moieties to stack with each other. The close stacking is much advantageous to the formation of π-dimers. In addition, the shortening of the bridged alkylene chains would give rise to a strong π-dimeric interaction. Actually, a preliminary study on [2.2]quinquethiophenophane (**4a**) with two ethylene chains revealed that it, unlike the nonstacked **2a**, can form a π-dimer readily.[18] However, the electronic absorption spectrum of the π-dimer is quite different in shape and wavelength from those previously observed for the dimeric quiquethiophenes **2b**−**e** as well as long oligothiophenes **1**. To clarify this inconsistency, we have made a systematical examination of a series of [*n*.*n*]quinquethiophenophanes (**4a**−**e**). This paper reports the syntheses, structures, spectroscopic properties, and π-dimeric interactions of these double-decker compounds.

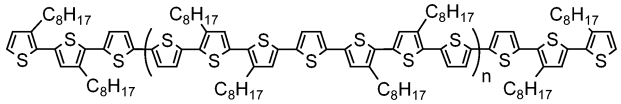
1, n = 0 – 6

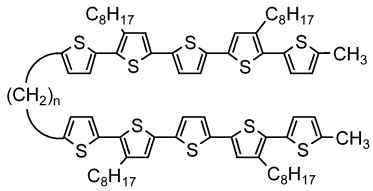
2a–e, n = 2 – 6

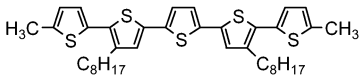
3

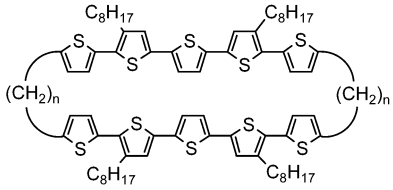
4a–e, n = 2 – 6

Results and Discussion

Syntheses. All the quinquethiophenophanes **4a**−**e** were synthesized using a combination of the Eglinton homocoupling reaction of ethynylbithiophenes and the subsequent sodium sulfide-induced cyclization reaction of the resulting diacetylene linkage for the construction of the oligothiophene skeleton.[15,19] Scheme 1 outlines the syntheses of [2.2]quinquethiophenophane (**4a**) and [3.3]quinquethiophenophane (**4b**). Treatment of 1,2-bis(3′-octyl-2,2′-bithien-5-yl)ethane (**5a**)[17] with 2 equiv of NBS gave the dibromo derivative **6a** in 89% yield, and the Sonogashira coupling reaction[20] of **6a** with trimethylsilylacetylene in the presence of catalytic $Pd(PPh_3)_4$ gave the bis(trimethylsilylethynyl) derivative **7a** (97% yield), which was then desilylated with potassium hydroxide to the ethynyl derivative **8a** (93% yield). An intermolecular double Eglinton homocoupling reaction of **8a** under dilution conditions gave the cyclic dimer **9a** (22% yield). The diacetylene parts of **9a** were converted to the thiophene rings by treatment with sodium sulfide to afford the desired [2.2]quiquethiophenophane (**4a**) (41% yield). [3.3]-

(13) Torrance, J. B.; Scott, B. A.; Welber, B.; Kaufman, F. B.; Seiden, P. E. *Phys. Rev. B* **1979**, *19*, 730−741.
(14) Graf, D. D.; Campbell, J. P.; Miller, L. L.; Mann, K. R. *J. Am. Chem. Soc.* **1996**, *118*, 5480−5481.
(15) (a) Nakanishi, H.; Sumi, N.; Aso, Y.; Otsubo, T. *J. Org. Chem.* **1998**, *63*, 8632−8633. (b) Sumi, N.; Nakanishi, H.; Ueno, S.; Takimiya, K.; Aso, Y.; Otsubo, T. *Bull. Chem. Soc. Jpn.* **2001**, *74*, 979−988.
(16) Nakanishi, H.; Sumi, N.; Ueno, S.; Takimiya, K.; Aso, Y.; Otsubo, T.; Komaguchi, K.; Shiotani, M.; Ohta, N. *Synth. Met.* **2001**, *119*, 413−414.
(17) Satou, T.; Sakai, T.; Kaikawa, T.; Takimiya, K.; Otsubo, T.; Aso, Y. *Org. Lett.* **2004**, *6*, 997−1000.
(18) Kaikawa, T.; Takimiya, K.; Aso, Y.; Otsubo, T. *Org. Lett.* **2000**, *2*, 4197−4199.
(19) (a) Beny, J.-P.; Dhawan, S. N.; Kagane, J.; Sundlass, S. *J. Org. Chem.* **1982**, *47*, 2201−2204. (b) Kagan, J.; Arora, S. K. *J. Org. Chem.* **1983**, *48*, 4317−4320.
(20) Sonogashira, K.; Tohda, Y.; Hagihara, N. *Tetrahedron Lett.* **1975**, 4467−4470.

Scheme 2 [a]

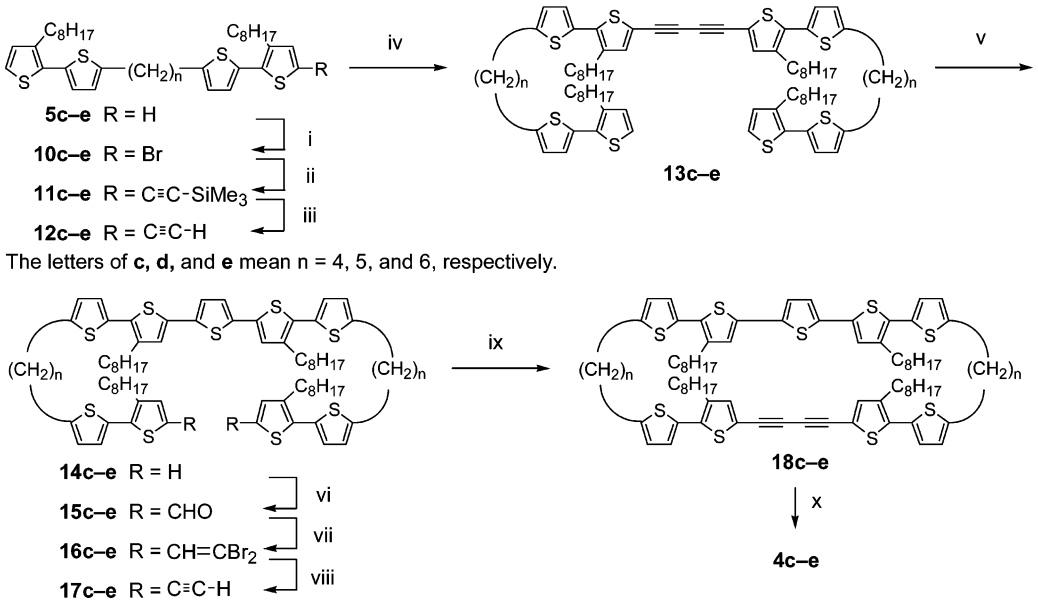

[a] Reagents and conditions: (i) NBS (56−61%); (ii) (trimethylsilyl)acetylene, $Pd(PPh_3)_4$, CuI, Et_3N (88−99%); (iii) KOH−MeOH (97%−quant.); (iv) $Cu(OAc)_2$, pyridine (84−98%); (v) $Na_2S{\cdot}H_2O$ (57−69%); (vi) $POCl_3$, DMF (55−68%); (vii) PPh_3, CBr_4 (45−97%); (viii) LDA, then H_2O (73−83%); (ix) $Cu(OAc)_2$, pyridine (76−86%); (x) $Na_2S{\cdot}H_2O$ (46−52%).

Quinquethiophenophane (**4b**) was similarly prepared starting with 1,3-bis(3′-octyl-2,2′-bithien-5-yl)propane (**5b**),[17] but the Eglinton homocoupling of **8b** to **9b** and the subsequent sodium sulfide-induced ring formation to **4b** proceeded in lower yields of 9% and 17%, respectively.

Although the yields of the Eglinton coupling reactions are relatively low, the synthetic route to **4a** and **4b** is straightforward. However, this approach is inapplicable to the synthesis of the higher homologues **4c**−**e**, because the key coupling reaction of the ethynyl derivatives **8** with a long alkylene chain under dilution conditions favored the formation of cyclic monomers than the desired cyclic dimers **9**, and the reaction under nondilution conditions resulted in the formation of rather cyclic oligomers and polymers. This forced us to take an alternative step-by-step coupling route, as shown in Scheme 2. Treatment of α,ω-bis(3′-octyl-2,2′-bithien-5-yl)alkanes (**5c**−**e**)[17] with 1 equiv of NBS led to the formation of the monobromo derivatives **10c**−**e**, which were successively converted to the trimethylsilylethynyl derivatives **11c**−**e** and then to the ethynyl derivatives **12c**−**e**. The Eglinton coupling of **12c**−**e** to the acyclic dimers **13c**−**e** and the following ring formation smoothly produced **14c**−**e**. The conversion of **14c**−**e** to **17c**−**e** could not be accomplished by the same procedure described above, because the first dibromination of **14c**−**e** at both terminal α-positions of the bithiophene parts failed due to difficult isolation of the products. Instead, the selective ethynylation was carried out by a combination of the Vilsmeier reaction and the Corey−Fuchs reaction.[19,21] The intramolecular Eglinton coupling reactions of **17c**−**e** under high dilution conditions proceeded in high yields, and the resulting diacetylenes **18c**−**e** were smoothly converted to the desired quinquethiophenophanes **4c**−**e**.

Molecular Structures. All the new compounds **4a**−**e** were definitely characterized by NMR, MS spectroscopic measurements, and elemental analyses. Table 1 compares the chemical shifts of the thiophene proton signals in the ^1H NMR spectra. The inside thiophene proton H_3 and H_4 signals of **4a**−**e** as compared to the corresponding signals of **3** demonstrate upfield shifts owing to the diamagnetic ring currents of the opposite thiophenes. This is usually seen for typical layered cyclophanes[22] and strongly supports double-decker structures for **4a**−**e**.

Table 1. NMR Chemical Shifts (δ) for Thiophene Protons of **3** and **4a**−**e** Measured in Deuteriochloroform[a]

compd	H_1	H_2	H_3	H_4
3	6.71	6.91	6.98	7.03
4a	6.76	6.92	6.94	6.88
4b	6.62	6.79	6.93	6.89
4c	6.68	6.89	6.92	6.89
4d	6.59	6.84	6.85	6.77
4e	6.67	6.87	6.95	6.94

[a] The thiophene protons of **3** and **4a**−**e** are numbered from the outside rings to the inside rings.

For such double-layered [*n.n*]heterophanes, there are generally two stacking conformations of anti and syn.[23] However, it is known that [2.2](2,5)thiophenophane (**19**) like [2.2]metacyclophane exists only in an anti stacking conformation,[24] as disclosed by its X-ray crystallographic analysis.[25] The rigid steplike conformation of **19** in solution was also confirmed by its ^1H NMR spectrum, which was characterized by a downfield shift (δ 6.72) of the thiophene proton signal as compared to that (δ 6.45) of 2,5-dimethylthiophene.[26] On the other hand, [3.3](2,5)-thiophenophane (**20**) exists as an equilibrium mixture of both anti and syn conformations in a ratio of 20:1.[27] As expected,

(21) Corey, E. J.; Fuchs, P. L. *Tetrahedron Lett.* **1972**, 3769−3772.

(22) Mitchell, R. H. *Cyclophanes*, Keehn, P. M., Rosenfeld, S. M., Eds.; Academic Press: New York, 1983; Vol. 1, Chapter 4.

(23) (a) Gault, I.; Price, B. J.; Sutherland, I. O. *Chem. Commun.* **1967**, 540−541. (b) Fletcher, J. R.; Sutherland, I. O. *Chem. Commun.* **1969**, 1504−1505. (c) Rosenfeld, S. M.; Keehn, P. M. *J. Chem. Soc., Chem. Comm.* **1974**, 119−120.

(24) Winberg, H. E.; Fawcett, F. S.; Mochel, W. E.; Theobald, C. W. *J. Am. Chem. Soc.* **1960**, *82*, 1428−1435.

(25) Pahor, N. B.; Calligaris, M.; Randaccio, L. *J. Chem. Soc., Perkin Trans. 2* **1978**, 42−45.

(26) Otsubo, T.; Mizogami, S.; Osaka, N.; Sakata, Y.; Misumi, S. *Bull. Chem. Soc. Jpn.* **1977**, *50*, 1841−1849.

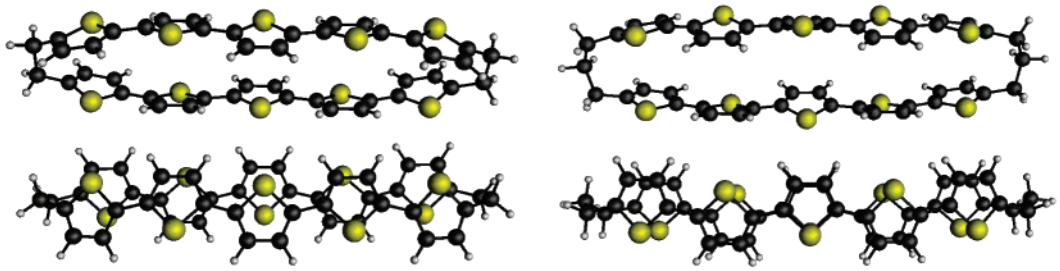

Figure 1. Calculated molecular structures of [2.2]quinquethiophenophane (**4a**) (side view, left and upper; top view, left and bottom) and [3.3]-quinquethiophenophane (**4b**) (side view, right and upper; top view, right and bottom). Octyl groups are omitted for the sake of simplicity.

the thiophene proton signal of the syn isomer with a face-to-face structure is characterized by an eminent upfield shift (δ 6.00). In this case, the thiophene proton signal of the anti isomer also shows a small upfield shift (δ 6.37) as compared to that of 2,5-dimethylthiophene. Provided that the oligothiophene sequences of **4a**−**e** keep all-trans linkage structures, as generally accepted for oligothiophenes, one may suppose that there are also both anti and syn stacking forms for the double-decker structures of **4a**−**e**. It is worthy noting that the chemical shifts of the outside thiophene proton H_1 and H_2 signals also reflect the anti or syn conformations of the thiophenophanes **4a**−**e**, although upfield or downfield shifts are much smaller than those observed for thiophenophanes **19** and **20**. The H_1 and H_2 signals of the [2.2]phane **4a** show small downfield shifts, as compared to the corresponding ones of **3**, and those of the [4.4]phane **4c** and the [6.6]phane **4e** are basically similar in chemical shifts. These compounds are grouped by even numbers for the bridged methylenes and supposed to adopt anti stacking conformations. On the other hand, the H_1 and H_2 signals of the [3.3]phane **4b** show marked upfield shifts. Similar upfield shifts are also observed for the [5.5]phane **4d**. The upfield shifts of these compounds with odd methylene numbers are understood by assuming syn stacking conformations. The alternate conformational changes of the homologues **4a**−**e** are speculated to arise from torsional strains in the bridged methylene linkages depending on the odd/even methylene numbers.

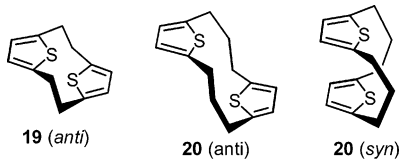

To verify the above conformational discussion based on the NMR spectra, we estimated the molecular structures of [2.2]-quinquethiophenophane (**4a**) and [3.3]quinquethiophenophane (**4b**) using the program GAMESS.[28] The geometries were fully optimized with restricted Hartree−Fock (RHF) at the 6-31G* level, and the results were visualized by MacMolPlt.[29] Figure 1 (left) shows the most stable structure for **4a**, in which the quinquethiophenes keep the sequence of the all-trans linkage and are stacked in the expected anti conformation. The anti structure is more stable by 26.0 kJ than the syn structure with the lowest calculated energy. On the other hand, the most favorable structure for **4b** is the syn conformation (Figure 1, right), which is, however, more stable only by 1.6 kJ than the anti structure. As seen from the top view of **4a**, all the thiophene rings, including even the outside thiophenes, are considerably located over the opposite thiophene rings, in contrast to the steplike structure of simple [2.2]thiophenophane **19**. This explains small downfield shifts observed for the H_1 and H_2 signals of **4a**, in contrast to the large downfield shift above-described for the thiophene protons of **19**. On the other hand, the top view of **4b** indicates that there are nearly complete overlaps for individual thiophene rings. This is in good agreement with the observation of upfield shifts for all thiophene proton signals. As seen from the side views, the quinquethiophene moieties of both **4a** and **4b** are widely bent, and accordingly, all the interlayer distances of the inside thiophene rings are over 4 Å. Only the bridged α-carbons and the neighboring β-carbons or sulfurs in the outside thiophene rings are located within van der Waals contacts of the opposite atoms. In **4a**, the close distances are 2.91 Å between α-carbons, 3.30−3.35 Å between the α-carbon and sulfur, and 3.45−3.56 Å between the β-carbon and sulfur. The sulfur−sulfur distances (3.64−3.67 Å) are nearly equal to double the van der Waals radius of sulfur (3.6 Å). On the other hand, in **4b**, the close distances are 3.30 Å between α-carbons and 3.46 Å between β-carbons. In this case, the sulfur−sulfur distances are 3.83−3.85 Å, which are farther than those in **4a**.

Electronic Spectra. As depicted in Figure 2, the electronic spectra of quinquethiophenophanes **4a**−**e** in dichloromethane are characterized by a broad $\pi-\pi^*$ absorption band and a structured emission band. Table 2 summarizes the absorption and emission maxima of **4a**−**e**, together with those of monomeric quinquethiophene **3**. When compared to that (416 nm) of **3**, the absorption bands of **4a**−**e** are at shorter wavelengths (λ_{max} 401−412 nm), and the absorption coefficients (ϵ 73 000−86 000) are much smaller than double that of **3** (ϵ 44 000). The blue shifts and reduced intensities of the absorption bands become marked with decreasing chain length, reflecting the interlayer distances of the stacking structures of **4a**−**e**. On the other hand, **4a**−**e** fluoresce at longer wavelengths than does **3**, and the emission intensities are considerably diminished. The opposite wavelength shifts of the absorption and emission bands are explained in terms of exciton−exciton coupling.[30] One should notice that the eminent reductions of the emission bands, unlike the case of the absorption bands, are observed for **4b**

(27) Miyahara, Y.; Inazu, T.; Yoshino, T. *Chem. Lett.* **1980**, 397−400.
(28) Schmidt, M. W.; Baldridge, K. K.; Boatz, J. A.; Elbert, S. T.; Gordon, M. S.; Jensen, J. H.; Koseki, S.; Matsunaga, N.; Nguyen, K. A.; Su, S.; Windus, T. L.; Dupuis, M.; Montgomery, J. A., Jr. *J. Comput. Chem.* **1993**, *14*, 1347−1363.
(29) Bode, B. M.; Gordon, M. S. *J. Mol. Graphics Mod.* **1999**, *16*, 133−138.
(30) (a) Katoh, T.; Inagaki, Y.; Okazaki, R. *Bull. Chem. Soc. Jpn.* **1997**, *70*, 2279−2286. (b) Cornil, J.; dos Santos, D. A.; Crispin, X.; Silbey, R.; Brédas, J. L. *J. Am. Chem. Soc.* **1998**, *120*, 1289−1299. (c) Cornil, J.; Beljonne, D.; Calbert, J.-P.; Brédas, J.-L. *Adv. Mater.* **2001**, *13*, 1053−1067.

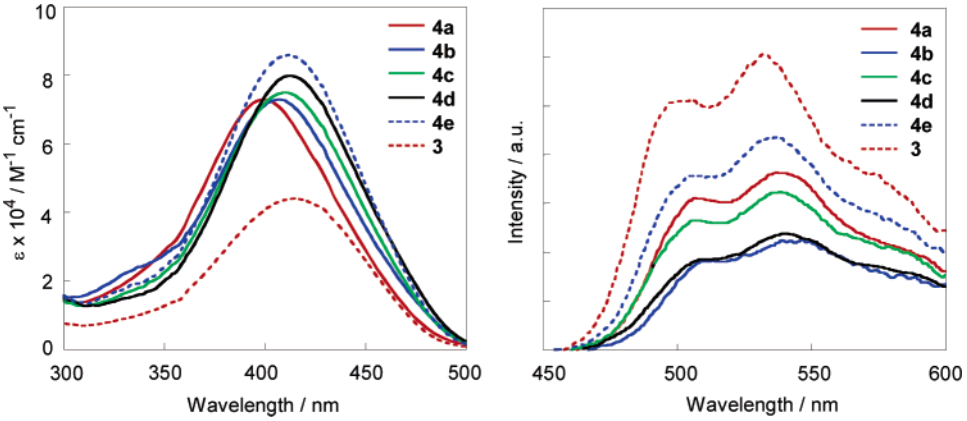

Figure 2. Electronic absorption spectra (left) and emission spectra (right) of **3** and **4a**−**e**. In the emission mesurement, the absorbances of all samples were kept constant.

Table 2. Band Maxima of Absorption and Emission Spectra[a] and Half-Wave Oxidation Potentials[b] of **3** and **4a**−**e**

	neutral		1e oxidation[c]:	2e oxidation[d]:		
compd	λ_{max}(abs)/nm[e]	λ_{max}(em)/nm	λ_{max}(abs)/nm	λ_{max}(abs)/nm	$E_{1/2}^1$/V	$E_{1/2}^2$/V
3	416 (44 000)	503, 533	752, 1408	902	0.31	0.53
4a	401 (73 000)	509, 540	410, 753, 1413	707, 924, 1399	0.25	0.64
4b	408 (73 000)	513, 548	446, 770, 1513	670, 1230	0.22	0.60, 0.73[f]
4c	410 (75 000)	508, 539	440, 762, 1407	692, 1187	0.28	0.65[g]
4d	413 (80 000)	509, 541	438, 761, 1411	691, 1181	0.26	0.65[g]
4e	412 (86 000)	508, 536	436, 763, 1406	619, 671sh,[h] 1087	0.27	0.64

[a] Electronic absorption and emission spectra were measured in dichloromethane. [b] Cyclic voltammetry was measured at a scan rate 100 mV/s in dichloromethane containing 0.1 M tetrabutylammonium hexafluorophosphate as a supporting electrolyte using platinum working and counter electrodes and a Ag/AgCl reference electrode. The redox potential of Fc/Fc^+ couple under these conditions is +0.51 V. Each wave corresponds to two-electron oxidation, unless otherwise stated. [c] Absorption spectra under one-electron oxidation with $FeCl_3$ indicate one neutral and two polaronic bands except only two polaronic bands for **3**. [d] Absorption spectra under two-electron oxidation with $FeCl_3$ indicate π-dimeric bands except a bipolaronic band for **3**. [e] Molar absorption coefficients are given in parentheses. [f] Split into two one-electron waves. [g] Set about splitting. [h] The low-energy band is structured.

and **4d**, whose structures are classified as the syn conformation. In addition, the largest red-shift of the emission band is observed for the second [3.3]phane **4b** rather than for the first [2.2]phane **4a** with the shortest bridged chains. Apparently, these results suggest the involvement of nonbonded electronic interactions in the excited states, besides exciton−exciton coupling. Considering that layered cyclophanes have been generally recognized as good excimer models,[31] we speculate that one of the interactions is presumably of an excimer type. The excimer type interaction well accounts for the remarkable emission quenching for the syn overlapped [3.3]phane **4b** and [5.5]phane **4d**. In addition, the observation of the largest spectral shift for **4b** in this series is coherent with the "Hirayama rule", that is, two chromophores connected by trimethylene groups form an intramolecular excimer most easily.[32,33]

***π*-Dimer Formation.** The controlled oxidation of **3** and **4a**−**e** with $FeCl_3$ in dichloromethane led to the successive formation of radical cation and dication species, which were monitored by vis/NIR spectroscopic measurements. According to the selection rule, as illustrated in Figure 3, two $\pi-\pi^*$-electronic transitions for polaron, one for bipolaron, and three for π-dimer are allowed.[34] As shown in Figure 4, the one-electron oxidation of **3** at room-temperature resulted in the disappearance of the neutral band at 416 nm and, instead, the appearance of two bands at 752 and 1408 nm, assignable to the P_1 and P_2 transitions, respectively, of the radical cation species (polaron). Further two-

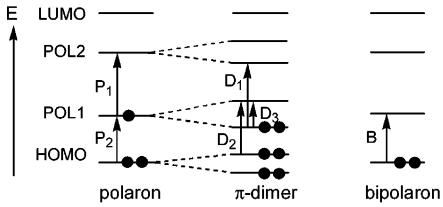

Figure 3. Energy transition diagrams of three oxidized species.

electron oxidation led to the appearance of only one band at 902 nm due to the dication species (bipolaron). When the one-electron oxidation spectrum of **3** was measured under cooling to 248 K, two additional bands appeared at the shorter wavelength sides (610−670 and 1084 nm) of the polaronic bands. This is due to the formation of π-dimer, and these two new bands are identified to the intrachain D_1 and D_2 transitions of π-dimer.[3]

The one-electron oxidation of [2.2]phane **4a** measured at room temperature showed three absorption bands (see Figure 5). The first band at 410 nm is due to the nonoxidized quinquethiophene. The remaining two bands (λ_{max} 753 and 1413 nm) are due to the oxidized quinquethiophene (polaron), and the absorption maxima are very similar to those of **3**. This clearly indicates that there is no or little electronic interaction between the neutral and polaronic species in the one-electron oxidation state of **4a**. Two-electron oxidation induces a spectral change to three absorption bands at λ_{max} 707, 924, and 1399 nm. The selection rule strongly suggests the formation of π-dimers. Considering the intensities, we assigned the first and second strong bands to the intrachain D_1 and D_2 transitions and the last weak band to the interchain D_3 transition. The formation

(31) Ferguson, J. *Chem. Rev.* **1986**, *86*, 957−982.
(32) Hirayama, F. *J. Chem. Phys.* **1965**, *42*, 3162−3171.
(33) Zachariasse, K.; Kühnle, W. *Z. Phys. Chem. N. Folge* **1976**, *101*, 267−276.
(34) Conil, J.; Brédas, J.-L. *Adv. Mater.* **1995**, *7*, 295−297.

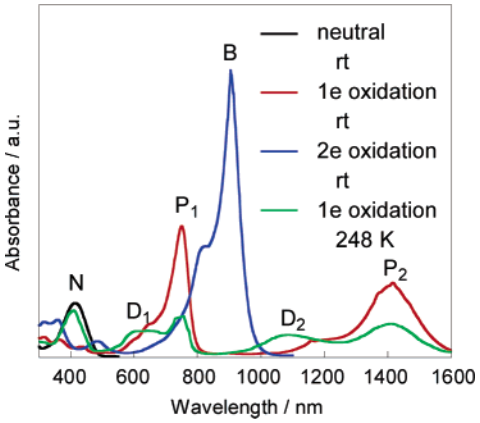

Figure 4. Electronic absorption spectra of **3** in dichloromethane in the neutral state and under one-electron oxidation at room temperature and at 248 K and two-electron oxidation at room temperature with $FeCl_3$. N, P, D, and B denote neutral, polaronic, π-dimeric, and bipolaronic bands, respectively.

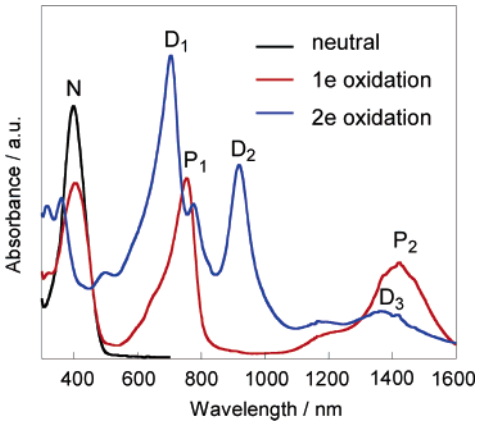

Figure 5. Electronic absorption spectra of **4a** in dichloromethane under controlled oxidation at room temperature with $FeCl_3$. N, P, and D denote neutral, polaronic, and π-dimeric bands, respectively.

of π-dimer species was strongly corroborated by the fact that a broad ESR signal with $g = 2.0022$ due to the polaron species formed under one-electron oxidation drastically disappeared under two-electron oxidation (Figure S1, left, of the Supporting Information). This ready π-dimerization of the two quinquethiophene polarons in **4a** is in sharp contrast to no intramolecular π-dimerization for **2a** as well as no intermolecular π-dimerization at room temperature for monomeric quinquethiophene **3**. Further three- and four-electron oxidation reactions of **4a** caused the appearance of a single peak at λ_{max} 779 nm, assignable to a bipolaronic band. A large blue shift of this band as compared to the bipolaronic band (902 nm) of **3** can be again explained by a strong exciton−exciton interaction.

Similar one-electron oxidation of [3.3]phane **4b** demonstrated two polaronic bands at λ_{max} 770 and 1513 nm together with a neutral band at 446 nm due to the nonoxidized quinquethiophene chromophore, as shown in Figure 6. Different from the case of the [2.2]phane **4a**, both the polaronic bands and the neutral band are markedly red-shifted as compared to the respective bands of **3**. These shifts are presumably due to an effective through-space electronic interaction between the oxidized quinquethiophene and the neutral one.[35] This is reminiscent of a general trend that [3.3]cyclophanes can effect stronger charge-transfer interactions than [2.2]cyclophanes.[36] Two-electron oxidation made a spectral change to two strong electron

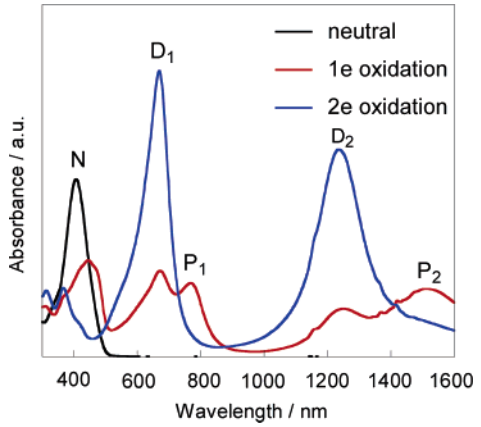

Figure 6. Electronic absorption spectra of **4b** in dichloromethane under controlled oxidation at room temperature with $FeCl_3$. N, P, and D denote neutral, polaronic, and π-dimeric bands, respectively.

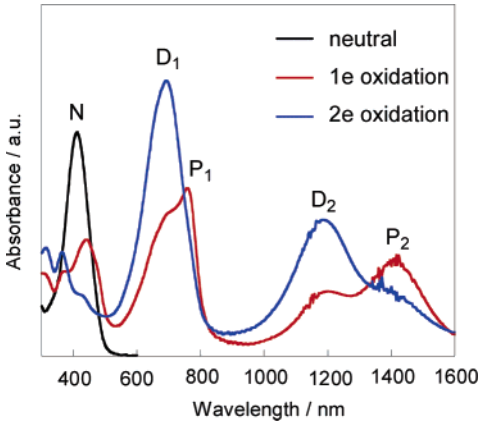

Figure 7. Electronic absorption spectra of **4c** in dichloromethane under controlled oxidation at room temperature with $FeCl_3$. N, P, and D denote neutral, polaronic, and π-dimeric bands, respectively.

transitions at 670 and 1230 nm. This spectrum is apparently unlike the π-dimeric spectrum of [2.2]phane **4a** with three transitions. However, the formation of π-dimer species under two-electron oxidation was again verified by complete disappearance of an ESR signal of the polaron species (see also Figure S1, right).

The π-dimeric spectrum of **4b** is quite similar to those previously observed for single-linked dimeric quinquethiophenes **2b**−**e** and can be understood by considering that the longer wavelength transition is red-shifted to conceal the third weak interchain transition. Surprisingly, the π-dimeric bands are partially detected even in the one-electron oxidation spectrum of **4b**. Apparently the π-dimer species of **4b** is highly stable.

The higher homologues **4c**−**e** upon successive oxidation showed the same spectral changes as seen for **4b** (Figure 7 for **4c**, Figure S2 for **4d**, and Figure S3 for **4e**). One-electron oxidation again caused the appearance of two polaronic bands,

(35) (a) Tsuchida, A.; Yamamoto, M. *J. Photochem. Photobiol. A* **1992**, *65*, 53−59. (b) Tsuchida, A.; Takamura, H.; Yamamoto, M. *Chem. Phys. Lett.* **1992**, *198*, 193−196. (c) Hotta, S.; Waragai, K. *J. Phys. Chem.* **1993**, *97*, 7427−7434. (d) Beljonne, D.; Cornil, J.; Sirringhaus, H.; Brown, P. J.; Shkunov, M.; Friend, R. H.; Brédas, J.-L. *Adv. Funct. Mater.* **2001**, *11*, 229−234. (e) Apperloo, J. J.; Janssen, R. A. J.; Malenfant, P. R. L.; Fréchet, J. M. J. *J. Am. Chem. Soc.* **2001**, *123*, 6916−6924.

(36) (a) Shinmyozu, T.; Inazu, T.; Yoshino, T. *Chem. Lett.* **1977**, 1347−1350. (b) Staab, H. A.; Herz, C. P. *Angew. Chem. Int. Ed. Engl.* **1977**, *16*, 799−801. (c) Haenel, M. W.; Flatow, A.; Taglieber, V.; Staab, H. A. *Tetrahedron Lett.* **1977**, 1733−1736. (d) Horita, H.; Otsubo, T.; Misumi, S. *Chem. Lett.* **1978**, 807−810.

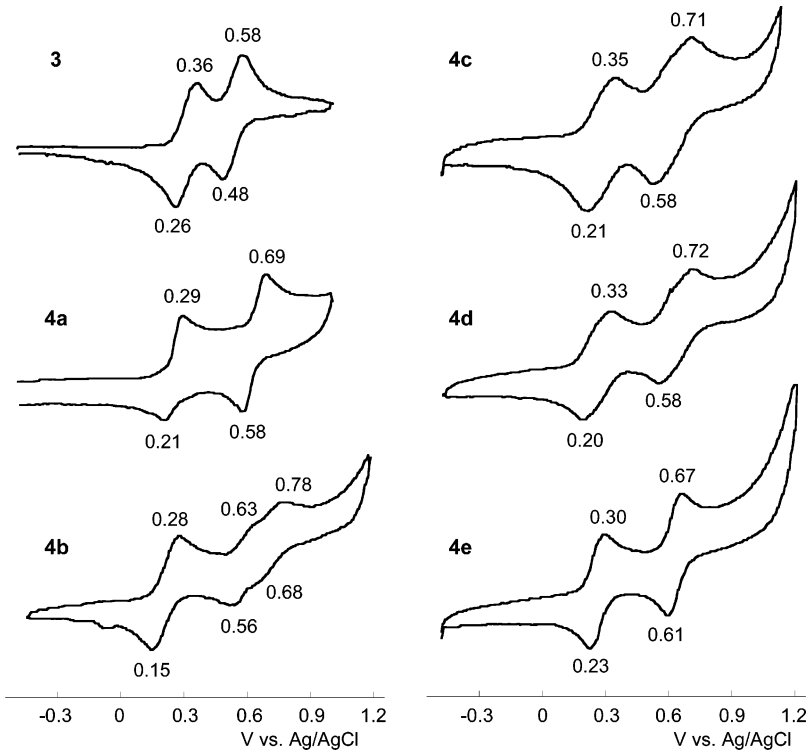

Figure 8. Cyclic voltammogram of **3** and **4a**−**e** in dichloromethane.

together with a small amount of π-dimeric bands. Two-electron oxidation predominantly gave two π-dimeric bands, but a small amount of polaronic bands remained. Consistent with this observation, the ESR signal due to the polaronic species did not completely disappear under two-electron oxidation (Figure S4 for **4c**). Evidently, these higher homologues cannot form π-dimers so easily as the [2.2]phane **4a** and the [3.3]phane **4b**.

A recent theoretical calculation on the structure and stability of quaterthiophene π-dimer proposed that it has an almost planar stacked structure with a ca. 3.1 Å interlayer distance and a large contact area.[37] When compared to the molecular structures of **4a** and **4b** in Figure 1, this means that the inside thiophene rings must approach more closely and overlap more effectively for π-dimerization. It is supposed that the [3.3]phane **4b** with syn conformation is more advantageous to such a structural change than the [2.2]phane **4a** with anti conformation, although the close interlayer distances are farther. The π-dimeric spectra of the [3.3]phane **4b** and higher homologues well explain that two broad absorption bands observed for doped polythiophenes[38] and doped long oligothiophenes[16] in the vis/NIR region principally originate from π-dimer species. The quite different π-dimeric spectrum of **4a** suggests that the two short bridging chains of **4a** force the π-dimer to take a constrained, strongly interactive structure.

Finally, it is worth mentioning that the π-dimeric bands of **4b**−**e** are closely related to the π-dimeric interactions. As seen in Table 2, the π-dimer of **4e** with the longest interlayer distance shows the low-energy band at nearly the same wavelength as the intermolecular π-dimer formed from **3**, and the bands of **4b**−**e** are red-shifted as the chain lengths decrease. In particular, the strongly associated π-dimer of **4b** shows the absorption maximum at 1230 nm, remarkably red-shifted as compared to the low-energy band (1087 nm) of **4e**. Evidently, the short bridged chains of **4b** are effective not only in the ready π-dimerization of quinquethiophenes but also in the strong π-dimeric interaction. Furthermore, the π-dimeric bands of **4b**−**e** are at longer wavelengths than the corresponding ones of the previously studied single-linked dimeric oligothiophenes **2b**−**e**: **2b**, λ_{max} 1193 nm; **2c**, 1112 nm; **2d**, 1095 nm; **2e**, 1086 nm.[17] This evidently indicates that double linkage of dimeric quinquethiophenes is more effective for π-dimeric interactions than single linkage.

Cyclic Voltammograms. The oxidation potentials provide helpful information on the electronic interactions between two quinquethiophenes in the oxidation states. The cyclic voltammograms of **3** and **4a**−**e** are shown in Figure 8, and the half-wave oxidation potentials are summarized in Table 2. The monomeric quinquethiophene **3** exhibits two reversible redox waves at $E_{1/2}$ = 0.31 and 0.53 V vs a Ag/AgCl standard in dichloromethane, each of which corresponds to one-electron oxidation. The [2.2]phane **4a** shows two similar reversible redox waves, but each wave corresponds to two-electron oxidation. The first half-wave oxidation potential (0.25 V) is lower than that of **3**, which is speculated to be principally induced by stabilization of the dicationic state due to π-dimerization of **4a**, as above-discussed. Presumably, a structural change for π-dimerization is quite faster than the voltammetric time scale. On the other hand, the second half-wave oxidation potential (0.64 V) of **4a** is much higher than that of **3**, indicating the retardation of the multioxidation steps by Coulombic repulsion in highly oxidized quinquethiophene species. This tendency becomes more pronounced for the [3.3]phane **4b**. The first wave further decreases up to $E_{1/2}$ = 0.22 V, thanks to higher stabilization for π-dimerization. One may notice that the separation (0.13 V) between the anodic peak and the counter cathodic peak

(37) Brocks, G. *J. Chem. Phys*. **2000**, *112*, 5353−5363.
(38) Harbeke, G.; Baeriswyl, D.; Kiess, H.; Kobel, W. *Phys. Scr*. **1986**, *T13*, 302−305.

slightly increases as compared to those of **3** (0.10 V) and **4a** (0.08 V). This suggests that the stabilization due to charge delocalization in the monocationic state also contributes to the apparent lowering of the first oxidation wave. The second wave is not only enhanced but also split into the two parts, $E_{1/2}$ = 0.60 and 0.73 V, by severe Coulombic repulsion. It is thus evident that the electrochemical multioxidation sequence of the quinquethiophenophane occurs stepwise. The remaining higher homologues **4c**−**e** also show lowering of the first waves and elevation of the second waves. The modest lowering of the first waves for **4c**−**e** as compared to those for **4a** and **4b** is consistent with the above-discussed chain-dependency for the ready π-dimerization of the quinquethiophenophanes. In addition, the second waves of **4c** and **4d** set about splitting.

Conclusions

We have here described the synthesis and properties of a series of [*n.n*]quinquethiophenophanes **4a**−**e**, which are very useful as π-dimer models of conductive polythiophenes. NMR spectroscopic studies have indicated that these compounds take double-decker structures with alternate anti and syn stacking fashions, depending on even or odd numbers of bridged methylenes. The different stacked structures of **4a** and **4b** have been corroborated by molecular structure calculations. Electronic spectral and voltammetric measurements have revealed that the two stacked quinquethiophenes of **4a**−**e** undergo marked nonbonded electronic interactions, such as exciton−exciton coupling and excimer type interaction in the neutral state, charge delocalization in the one-electron oxidation state, and π-dimeric interaction in the two-electron oxidation state. In addition, it is found that the closer stacking of the quinquethiophanes as seen for **4a** and **4b** induces the ready formation of π-dimers with strong electronic interactions. The observed electronic bands of π-dimers are much perturbed by π-dimeric interactions. The π-dimeric spectrum of the most closely stacked [2.2]phane **4a** allows the appearance of three electron transitions inherent in a π-dimer. Presumably, the two short bridging chains of **4a** force the π-dimer to take a constrained, strongly interactive structure. In contrast, the π-dimeric spectra of **4b**−**e** are characterized by only two strong intrachain electron transitions with red-shifts depending on the interlayer distances. Since these higher homologues presumably undergo conformational changes for π-dimerization rather flexibly than **4a**, they can be thought to behave as better π-dimer models for conductive polythiophene. Actually, the π-dimeric spectra of **4b**−**e** well explain that two broad absorption bands observed for doped polythiophene in the vis/NIR region principally originate from π-dimer species.

Acknowledgment. This research was partly supported by Grants-in-Aid of Scientific Research (Category A, No. 1330405 and Priority Areas of Molecular Conductors, No. 15073218) from the Ministry of Education, Culture, Sports, Science and Technology, Japan.

Supporting Information Available: All experimental details for the syntheses of [*n.n*]quinquethiophenophanes (**4a**−**e**) and reference compound **3**, ESR spectra of oxidized **4a**−**e**, and electronic absorption spectra of oxidized **4d** and **4e**. This material is available free of charge via the Internet at http://pubs.acs.org.

JA050783U